The Company of **Biologists**

SHORT COMMUNICATION

Calibrated microphone array recordings reveal that a gleaning bat emits low-intensity echolocation calls even in open-space habitat

Léna de Framond[1,*,**], Thejasvi Beleyur[1,2,3,*], Daniel Lewanzik[1,‡,¶] and Holger R. Goerlitz[1,§,¶]

ABSTRACT

Echolocating bats use ultrasound for orientation and prey capture in darkness. Ultrasound is strongly attenuated in air. Consequently, aerial-hawking bats generally emit very intense echolocation calls to maximize detection range. However, call levels vary more than tenfold (>20 dB) between species and are tightly linked to the foraging strategy. The brown long-eared bat (*Plecotus auritus*) is a primarily gleaning, low-amplitude species that may occasionally hawk airborne prey. We used state-of-the-art calibrated acoustic 3D-localization and automated call analysis to measure *P. auritus*' source levels. *Plecotus auritus* emits echolocation calls of low amplitude (92 dB rmsSPL re. 20 µPa at 10 cm) even while flying in open-space. While *P. auritus* thus probably benefits from delayed evasive manoeuvres of eared insects, we propose that low-amplitude echolocation did not evolve as an adaptive countermeasure, but is limited by morphological constraints.

KEY WORDS: Brown long-eared bats, Source level, Evolutionary arms race, *Plecotus*, Gleaning, Call amplitude

INTRODUCTION

The information that an animal can obtain about its environment is limited by the maximum detection range over which it can detect sensory stimuli. This detection range is determined by properties of the environment, the stimulus and the sensory system (Dusenbery, 2001). The 'sensory drive hypothesis' postulates that both signals and sensory systems are adapted to an animal's typical environment to maximize information acquisition (Cummings and Endler, 2018; Endler, 1992).

Echolocating bats perceive their surroundings through sound. Open-space foraging species maximize detection range by emitting very high-intensity calls with source levels often above the human pain threshold [120–140 dB peak-equivalent sound pressure level (peSPL) re. 20 µPa at 10 cm distance to the mouth; Boonman et al., 2013; Fujioka et al., 2014; Goerlitz et al., 2020; Holderied and von

Helversen, 2003; Holderied et al., 2005; Surlykke and Kalko, 2008]. Morphological and behavioural adaptations, such as large ears (Coles et al., 1989; Wotton et al., 1995) and ear movements (Yin and Müller, 2019), aid in prey detection. Nevertheless, their detection range is limited to between a few metres to tens of metres (Stilz and Schnitzler, 2012), strongly depending on call frequency, amplitude, object size and reflective properties (Møhl, 1988).

In contrast to open-space foraging bats, some species catch prey from vegetation or the ground ('gleaning') and typically emit low-amplitude calls, more than 10 times (>20 dB) fainter than those of aerial-hawking species (Corcoran and Conner, 2017; Goerlitz et al., 2010; Holderied et al., 2011; Seibert et al., 2015; Stidsholt et al., 2022). Using low-amplitude echolocation during gleaning avoids masking of the faint prey-generated sounds and prey echoes by loud vegetation echoes and is regarded as an adaptation to foraging close to background structures (Jakobsen et al., 2013; Surlykke et al., 2009). For example, the desert long-eared bat (*Otonycteris hemprichii*, plecotine tribe) emits low-amplitude echolocation calls during ground gleaning but increases call amplitude drastically when flying in the open (Hackett et al., 2014), suggesting that the shorter detection distance of low-amplitude calls is costly during aerial hawking. In contrast, the Western barbastelle bat (*Barbastella barbastellus*) and the North-American Townsend's big-eared bat (*Corynorhinus townsendii*) emit low-amplitude calls (∼100 dB peSPL at 10 cm) in open space (Corcoran and Conner, 2017; Lewanzik and Goerlitz, 2018, 2021). Although this low-amplitude strategy strongly limits these bats' detection distance for prey, it provides an advantage over eared moths, which fail to hear their predator and to initiate evasive flight (Corcoran and Conner, 2017; Goerlitz et al., 2010; Lewanzik and Goerlitz, 2018).

Brown long-eared bats (*Plecotus auritus*), like most other plecotine species, glean prey off vegetation and emit low-amplitude calls when gleaning (Anderson and Racey, 1991; Waters and Jones, 1995). The high proportion of eared-moths in their diet (∼25–40%; Rydell, 1989; Shiel et al., 1991; Vesterinen et al., 2018) and observations of hawking in the lab (Anderson and Racey, 1991) suggest that *P. auritus* might also hawk prey in open space (Dietz and Kiefer, 2016). To date, it is unknown whether they emit low-intensity calls when flying in open space – like the barbastelle and Townsend's big-eared bat – or high-intensity calls – like desert long-eared bats.

To close this gap of knowledge, we measured call source levels of wild *P. auritus* flying freely in their natural open-space habitat. We show that *P. auritus* emit low-intensity calls in open space, and discuss hypotheses about the evolutionary drivers underlying low-intensity echolocation.

[1]Acoustic and Functional Ecology, Max Planck Institute for Ornithology, 82319 Seewiesen, Germany. [2]Department of Biology, University of Konstanz, 78464 Konstanz, Germany. [3]Centre for the Advanced Study of Collective Behaviour, University of Konstanz, 78464 Konstanz, Germany.
*Present address: Acoustic Communication and Urban Ecology Group, Max Planck Institute for Biological Intelligence, 82319 Seewiesen, Germany. ‡Present address: Leibniz Institute for Zoo and Wildlife Research, 10315 Berlin, Germany. §Present address: Acoustic and Functional Ecology, Max Planck Institute for Biological Intelligence, 82319 Seewiesen, Germany.
¶Shared last author

**Author for correspondence (lena.framond@bi.mpg.de)

L.d.F., 0000-0002-5507-7668; T.B., 0000-0001-5360-4383; D.L., 0000-0003-3305-6556; H.R.G., 0000-0002-9677-8073

MATERIALS AND METHODS
Field recordings

We caught 10 (8 males, 2 females) brown long-eared bats, *Plecotus auritus* (Linnaeus 1758), with mist-nets on 21 August 2019, next to

Journal of Experimental Biology

1

a large bat colony at Silberberg, Eastern Bavaria, Germany. Bats were briefly kept in cloth bags. Within ~10–15 min, we released bats individually from the hand at ~10 m distance to a microphone array. Five of the bats flew towards the microphone array, allowing us to record their echolocation call sequences, which we used for subsequent reconstruction of their spatial positions and call analysis. The array consisted of four microphones (FG-O, Avisoft Bioacoustics, Glienicke, Germany) arranged in a planar symmetrical star-shaped pattern, with one central microphone surrounded by three microphones at 60 cm distance and 120 deg angular separation. The microphone array was positioned on the top of a small hill, free of trees, so that the bats were flying in open surroundings. Audio was recorded via a USG-416H soundcard and Recorder software (Avisoft Bioacoustics) at 500 kHz sampling rate and 16-bit resolution. Ambient temperature, relative humidity and atmospheric pressure were logged every 2 min during the recording session (Kestrel 4000, Nielsen-Kellerman, Boothwyn, PA, USA).

Flight path reconstruction and call analysis

We used custom-written software (TOADSuite, by Peter Stilz; Hügel et al., 2017; Lewanzik et al., 2019) for MATLAB 2007b (The MathWorks Inc., Natick, MA, USA) to calculate the bat's 3D position for each emitted call, and to analyse each call's acoustic properties as emitted by the bat. First, all recordings were filtered (20–90 kHz fourth-order elliptic bandpass filter, 0.1 dB peak-to-peak ripple, 40 dB minimum stopband attenuation) and calls were detected on the central microphone above a fixed threshold of −35 dB full scale (FS, i.e. relative to the maximum recordable level). Second, for each call, we measured the time-of-arrival difference between the central and each peripheral microphone by cross-correlation, and calculated the bat's 3D position at call emission. We displayed all detected bat positions (N=144) and their corresponding call waveforms and spectrograms on a graphical user interface to manually combine positions into flight trajectories and to visually control data quality. We manually excluded outlier positions (that did not align well with or were far off the other positions, N=16), and automatically excluded all positions of calls with a duration <1 ms (i.e. shorter than typical species-specific echolocation calls) or >8 ms (i.e. twice as long as typical echolocation calls; Russ, 2012). The >8 ms calls were measurement errors due to low signal to noise ratio (<15 dB, we manually checked all these calls; see Supplementary Materials and Methods; N=30 excluded calls). Finally, 98 calls remained for the final analysis.

To analyse the acoustic call parameters as emitted by the bat (at 10 cm distance from its mouth), we first reconstructed the emitted waveform of each detected call by correcting for microphone characteristics and sound attenuation on the way to the microphone. The microphone's frequency response and sensitivity were previously measured by recording white noise and pure tones in comparison to a calibrated measuring microphone (for details see Supplementary Materials and Methods). We calculated each call's recorded amplitude and phase spectrum with a fast Fourier transformation (FFT), corrected the amplitude spectrum for the microphone's frequency response, for frequency- and distance-dependent atmospheric attenuation at the local weather conditions (Goerlitz, 2018), and for the distance-dependent geometric attenuation, and then back-calculated the compensated waveform with an inverse FFT. We used the reconstructed source waveform to calculate the call's duration (at −12 dB below the peak of the call's envelope smoothed with a moving average of 0.2 ms) and apparent source level (aSL). For better comparability with other studies, we

calculated the apparent source level both as peSPL (i.e. a measure of the call's peak-to-peak amplitude; Burkard, 2006) and as root-mean-square sound pressure level (rmsSPL, i.e. a measure of the call's average amplitude). The peSPL value was calculated from the envelope of the call waveform, and the rmsSPL value as the root-mean-square of the waveform within the −12 dB call duration criterion. All sound pressure levels are referenced to 20 µPa and 10 cm distance to the bat's mouth. The aSL underestimates the real or 'on-axis' source level as the bats' flight and sonar beam direction are not always oriented towards the microphone. To estimate the real, on-axis source level, we calculated the 95th percentile of all aSL values per trajectory. This method is less likely to be influenced by outliers than calculating the mean of the 10% most intense calls or taking the maximum value per trajectory. A single very large value would not change the 95th percentile but would have a substantial impact on the mean or maximum (Holderied and von Helversen, 2003; Surlykke and Kalko, 2008). We further calculated each call's peak frequency (frequency with maximum amplitude of the average spectrum) and lowest frequency (lowest frequency at −12 dB below the peak frequency's amplitude) from the time-averaged call spectrogram (2000 FFT of 100 samples with Hann window, 95% overlap) derived from the compensated call waveform. To check whether the bats altered their echolocation to the presence of the microphone array, we fitted a linear mixed effect model (package *rstanarm* version 2.21.3, R version 4.2.2) on call duration over distance. We checked for the typical call duration decrease during object approach, limiting the analysis to calls within 3 m of the array, where we expected the strongest change in call parameters. The model was fitted in a Bayesian framework (4 chains of 5000 iterations, warmup 2500 iterations, default uninformative flat priors) with log(call duration) as response variable, distance to the central microphone as fixed effect, and bat identity as a random effect. We checked that the chains converged properly by inspecting caterpillar plots, R-hats and effective sample sizes, and assessed model fit using posterior predictive plots (https://cran.r-project.org/web/packages/bayesplot/vignettes/graphical-ppcs.html). We used the 2.5th and 97.5th percentile from 1000 posterior draws to calculate 95% credible intervals (CrI).

Accuracy of 3D localization and source-level calculations

We performed two calibration measurements to determine the accuracy of our acoustic tracking system for calculating (i) the 3D-coordinates of bats and (ii) the (apparent) source levels of bat calls. We broadcasted six types of synthetic signals from a custom-built Polaroid speaker placed at 45 different positions relative to the microphone array (3 azimuthal directions×3 elevational directions×5 distances ranging from 3 to 10 m). We analysed the recordings with TOADSuite in the same way as we analysed bat field recordings. We then compared the loudspeaker positions and amplitudes as calculated by TOADSuite to the known spatial positions and previously measured real source levels. The detailed procedures are described in the Supplementary Materials and Methods.

RESULTS AND DISCUSSION

Using a fully calibrated microphone array, we show that wild *P. auritus* flying in an open environment emit echolocation calls with low source level of only 90–99 dB rmsSPL (93–104 dB peSPL) re. 2 µPa at 10 cm distance. Calibrations showed that our system measures amplitude correctly independent of call duration, shape or distance to the array. Our calculated sound source positions showed no systematic error (mean distance error of −0.5% of the

real distance, range −9.4–10.9%; Fig. 1) and were not affected by azimuth, elevation, call duration or call shape (Fig. 1; Fig. S1). The localization error increased with increasing loudspeaker distance (Fig. 1), probably due to lower signal-to-noise ratio (SNR). Call frequency and duration were estimated accurately for playback signals having a SNR >20 dB (Fig. S1). Measured source levels were slightly lower than the expected values, with small mean differences for peak values (mean±s.d.: −1.1±1.7 dB) and somewhat larger differences for rms values (–4.2±1.5 dB; Fig. 1). For more details, see Supplementary Materials and Methods.

We analysed 98 calls of five *P. auritus* flying in a natural open environment (Fig. 2; Fig. S2). We present the median of individual medians along with the range of medians (see Table S1 for individual call data). The calls had a median duration of 2.5 ms (range 1.9–2.8 ms), a median peak frequency of the first harmonic of 37.8 kHz (31.7–39.0 kHz) and a median lowest frequency (−12 dB below peak frequency) of 26.5 kHz (22.2–28.2 kHz; Fig. 3). To estimate real source levels (SL), accounting for the high call directionality and that the call's axis is not necessarily pointing to the microphone, we calculated the 95th percentile of all aSL values per individual. The median (minimum−maximum of individual medians) SL across individuals was 88 dB rmsSPL (86–95 dB rmsSPL) and 94 dB peSPL (92–103 dB peSPL) (Fig. 3C). When adding 4 dB or 1 dB to correct for our system's slight underestimation of the rmsSPL and peSPL, respectively

(Fig. 1), *P. auritus* emitted calls with a median source level of 92 dB rmsSPL (90–99 dB rmsSPL) and 95 dB peSPL (93–104 dB rmsSPL). Previous studies estimated 89 and 97 dB peSPL for two individuals flying in a flight room (Waters and Jones, 1995) and 79 dB rmsSPL in a wind tunnel (Jakobsen et al., 2018). Although bats commonly call with lower levels in confined versus in open spaces (Brinkløv et al., 2010; Surlykke and Kalko, 2008), we show that *P. auritus* also emit low-amplitude echolocation calls when flying in open spaces in their natural habitat.

Despite potential methodological challenges, we are confident that we measured typical source levels of *P. auritus* in open space. The apparent increase in source level with distance to the microphone (Fig. 3D) is a recording bias rather than a behavioural response. Intense calls are detected over longer distances than fainter calls. The constant call durations close to the array [mean posterior estimate β=0.057, 95th percentile posterior CrI [−0.091, 0.199], which is an increase of 0.2 ms (10%) over 3 m on average] further confirms that the array did not induce a behavioural artefact. For comparison, common pipistrelles almost double their initial call duration over the same distance (analysis not shown, data from de Framond et al., 2023). While hand-released bats sometimes initially emit atypical echolocation calls (Szewczac, 2004), they soon return to typical echolocation (Obrist and Boesch, 2018) only 5 m post-release (Kohles et al., 2020). We recorded the bats >5 m post-release, so calls should have normalized. Echolocation calls are directional and not always oriented towards the array, which causes underestimated source levels. We thus present the 95th percentile of all echolocation call amplitudes per individual, which is a reliable method to estimate on-axis source levels (Holderied and von Helversen, 2003; Surlykke and Kalko, 2008).

Brown long-eared bat source levels are ∼10 dB lower than those of related low-amplitude species (Corcoran and Conner, 2017; Goerlitz et al., 2010; Lewanzik and Goerlitz, 2018; Seibert et al., 2015). In contrast, the echolocation call levels of aerial-hawking bats in open space are typically 10–100 times (20–40 dB) higher (Boonman et al., 2013; Fujioka et al., 2014; Goerlitz et al., 2020; Holderied and von Helversen, 2003; Holderied et al., 2005; Surlykke and Kalko, 2008). As call level determines the range over which bats can detect obstacles and prey (Goerlitz et al., 2010; Stidsholt et al., 2021), maximizing sensory range probably drove the evolution of high call levels in open-space foragers, up to the physiological limit (Currie et al., 2020). In comparison, the lower source levels of *P. auritus* severely limit their sensory range (Goerlitz et al., 2010), which begs the question of its adaptive value.

One advantage of using low source levels in open environments might unfold in a predator–prey context (Goerlitz et al., 2010). Many moths and other insects possess ears (Kawahara et al., 2019; Ter Hofstede and Ratcliffe, 2016) that enable them to detect bats and initiate evasive responses (Goerlitz et al., 2020; Roeder and Treat, 1957). Low-amplitude 'stealth' echolocation enables bats to successfully catch eared prey (Goerlitz et al., 2010; Ter Hofstede and Ratcliffe, 2016) and was thus presented as an adaptation to moth hearing ('coevolution hypothesis'; Conner and Corcoran, 2012; Fenton and Fullard, 1979; Goerlitz et al., 2010; Surlykke, 1988). In contrast, we argue here that the low source level of *P. auritus* is an adaption to a gleaning foraging strategy ('habitat adaptation hypothesis'; Lewanzik and Goerlitz, 2018) rather than to moth hearing. Morphological limitations caused by their nasal call emission may also limit a substantial increase of source levels in open environments.

Two lines of evidence support the habitat adaptation hypothesis. First, *P. auritus* are aerodynamically adapted for slow and
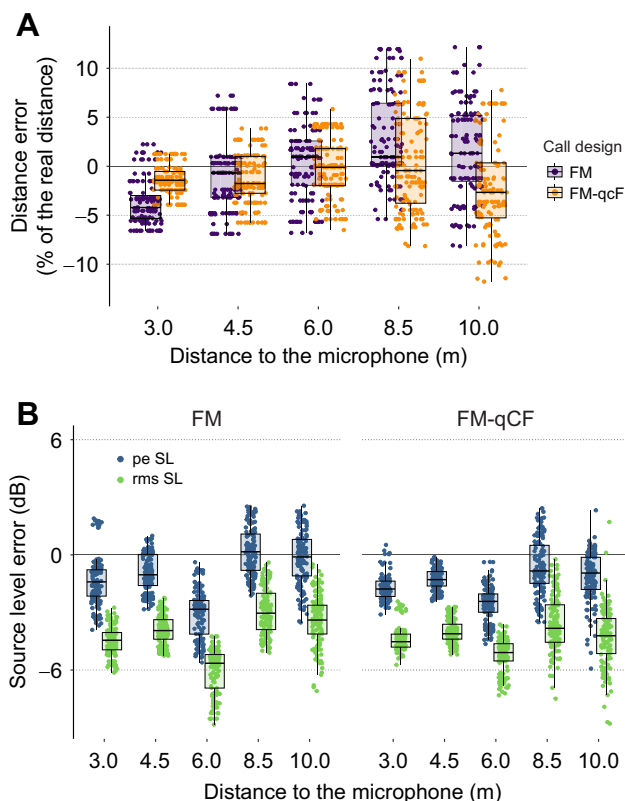

Fig. 1. Accuracy of distance and source-level measurements with a star-shaped four-microphone array and TOADSuite. Distance (A) and source level (B) error (i.e. difference between real and measured value) as a function of distance to the central microphone, and call shape (FM, frequency modulated; FM-qCF, frequency modulated with a quasi-constant frequency component). Source levels are presented as peak equivalent (pe SL) and root mean square (rms SL) values (B). Raw data (N=1374) are shown behind boxplots (median, quartiles and 95th percentiles).
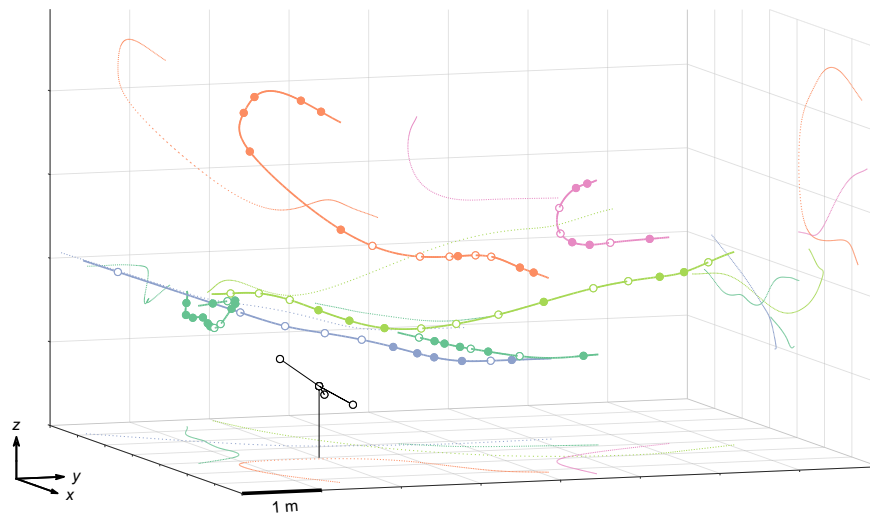
Fig. 2. Three-dimensional trajectories of all five bats whose calls (*N*=98) were analysed. Filled circles: included calls; open circles: position of calls that were excluded from acoustic analysis. Dotted lines are the projections of the trajectories on the 2D planes. Different colours correspond to different bats (see also Fig. 3). The microphone array is shown in black.

manoeuvrable flight (Norberg et al., 1987). This is necessary to glean prey in cluttered habitats but disadvantageous when hunting flying prey in open spaces, suggesting that the brown long-eared bat is (still) a primarily gleaning species. For gleaning bats, low-amplitude echolocation prevents the masking of faint prey sounds and prey echoes by intense vegetation echoes (Jacobs and Bastian, 2016). Hence, it seems most plausible that low source levels evolved in a gleaning context as adaptation to cluttered habitats. *Plecotus auritus* may have secondarily exploited their acoustic inconspicuousness for aerial hunting of eared moths, which

might explain the substantial proportion of eared moths in their faeces (Andriollo et al., 2019). Such flexible foraging strategies and even foraging niche transitions are common in bats (Arlettaz et al., 2001; Clare et al., 2014; Lewanzik and Goerlitz, 2021; Morales et al., 2019; Ratcliffe and Dawson, 2003).

Second, *P. auritus* emit their calls nasally, in contrast to the oral call emission of high-amplitude aerial-hawking vespertilionid bats. Increasing call source levels is challenging for nasal emitters (Brinkløv et al., 2010, 2011). Only rhinolophid and hipposiderid bats emit high source levels nasally using highly specialized nasal
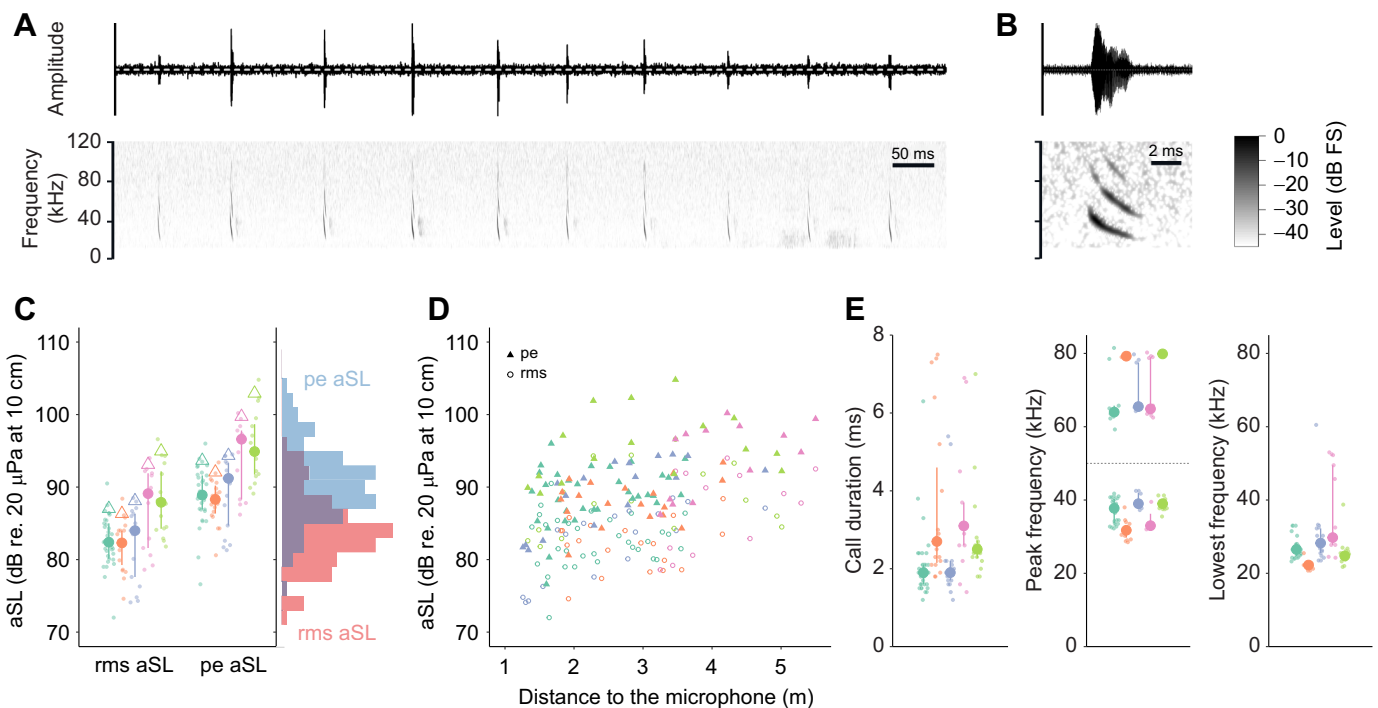

Fig. 3. Spectrogram and call parameters of five brown long-eared bats. (A,B) Waveforms (top) and spectrograms (bottom) of a 1 s call sequence (A) and a single call (B). FS, full scale. (C) Root mean square (rms) and peak equivalent (pe) apparent source level (aSL) of all analysed calls. Medians (large circles), quartiles (bars) and 90th percentiles (triangles) are shown along with raw data (small circles) per individual bat (colour coded). The histogram on the right shows overall aSL distributions. (D) aSL as a function of the distance to the central microphone. (E) Duration, peak frequency and lowest frequency of all analysed calls. Median and quartiles (large circles and solid lines) and individual calls (small circles) are shown per individual (colour coded). Call duration: the higher values probably include some trailing echoes and/or noise. Peak frequency: medians and quartiles were calculated separately for data below and above 50 kHz, to obtain peak frequencies in the first and second harmonic, respectively (separated by a grey dotted line at 50 kHz). The lack of peak frequencies around 70 kHz in the second harmonic probably originates from a not fully compensated dip in microphone sensitivity around 70 kHz.

cavities and skulls (Pedersen, 1998; Pedersen and Müller, 2013). Hence, we suggest that *P. auritus* are constrained to low source levels during echolocation. This does not exclude that they could use oral emission to emit loud social calls (as described by Ahlén, 1981). Little is known about these calls, including their source level. The physiological limit to the source levels caused by nasal emission is further supported by one other behaviourally flexible and orally emitting species that dramatically increases source levels (by more than 30 dB) – *Myotis myotis* – and possibly in *O. hemprichii* (no data on emission mode), which increases source level by more than 50 dB when switching from gleaning to aerial hawking (Hackett et al., 2014; Holderied et al., 2011; Stidsholt et al., 2021). Apparently, emitting high source levels during aerial captures is beneficial also for species that otherwise use low source levels when gleaning. Hence, we argue that morphological constraints probably prevent *P. auritus* from emitting high-intensity echolocation calls. Any selection pressure towards high source levels in *P. auritus* has probably been too low because they fly and forage mostly in cluttered environments, and this gives them an advantage in terms of catching eared prey.

In summary, we provide the first data on call source levels in free-flying *P. auritus* and show that – in contrast to some other low-amplitude gleaning species – they do not increase call amplitude when flying in open habitats. Their low call source level is probably an ancestral adaptation to their gleaning strategy. Their nasal call emission probably prevents them from substantially increasing source levels when flying in open environments. We suggest that this putative limitation is beneficial for hawking eared prey in the open air. The morphological limitation scenario contrasts the evolutionary arms-race scenario, in which low-intensity echolocation is a counter-measure to the evolution of ears in prey insects (Goerlitz et al., 2010). Further empirical data on echolocation call parameters, call emission modes, foraging styles and habitat use, as well as ancestral state analyses, are needed to disentangle the evolutionary drivers of extant low-amplitude echolocation.

Competing interests
The authors declare no competing or financial interests.

Author contributions
Conceptualization: H.R.G.; Methodology: T.B., D.L., H.R.G.; Validation: L.d.F., T.B.; Formal analysis: L.d.F.; Investigation: L.d.F., T.B., D.L.; Resources: H.R.G.; Data curation: L.d.F.; Writing - original draft: L.d.F., D.L., H.R.G.; Writing - review & editing: L.d.F., T.B., D.L., H.R.G.; Visualization: L.d.F., T.B., H.R.G.; Supervision: D.L., H.R.G.; Project administration: H.R.G.; Funding acquisition: H.R.G.

Data availability
Call recordings and the extracted acoustic parameters can be found at the Zenodo online repository: https://doi.org/10.5281/zenodo.7414956

ECR Spotlight
This article has an associated ECR Spotlight interview with Léna de Framond.

References

Ahlén, I. (1981). *Identification of Scandinavian Bats by their Sounds*. Uppsala, Sweden: Swedish University of Agricultural Sciences, Department of Wildlife Ecology.

Anderson, E. M. and Racey, P. A. (1991). Feeding behaviour of captive brown long-eared bats, *Plecotus auritus*. *Anim. Behav.* **42**, 489-493. doi:10.1016/S0003-3472(05)80048-X

Andriollo, T., Gillet, F., Michaux, J. R. and Ruedi, M. (2019). The menu varies with metabarcoding practices: a case study with the bat *Plecotus auritus*. *PLOS ONE* **14**, e0219135. doi:10.1371/journal.pone.0219135

Arlettaz, R., Jones, G. and Racey, P. A. (2001). Effect of acoustic clutter on prey detection by bats. *Nature* **414**, 742-745. doi:10.1038/414742a

Boonman, A., Bar-On, Y. and Yovel, Y. (2013). It's not black or white-on the range of vision and echolocation in echolocating bats. *Front. Physiol.* **4**, 248. doi:10.3389/fphys.2013.00248

Brinkløv, S., Kalko, E. K. and Surlykke, A. (2010). Dynamic adjustment of biosonar intensity to habitat clutter in the bat *Macrophyllum macrophyllum* (Phyllostomidae). *Behav. Ecol. Sociobiol.* **64**, 1867-1874. doi:10.1007/s00265-010-0998-9

Brinkløv, S., Jakobsen, L., Ratcliffe, J. M., Kalko, E. K. V. and Surlykke, A. (2011). Echolocation call intensity and directionality in flying short-tailed fruit bats, *Carollia perspicillata* (Phyllostomidae). *J. Acoust. Soc. Am.* **129**, 427-435. doi:10.1121/1.3519396

Burkard, R. (2006). Calibration of acoustic transients. *Brain. Res.* **1091**, 27-31. doi:10.1016/j.brainres.2006.02.132

Clare, E. L., Goerlitz, H. R., Drapeau, V. A., Holderied, M. W., Adams, A. M., Nagel, J., Dumont, E. R., Hebert, P. D. N. and Brock Fenton, M. B. (2014). Trophic niche flexibility in *Glossophaga soricina*: how a nectar seeker sneaks an insect snack. *Funct. Ecol.* **28**, 632-641. doi:10.1111/1365-2435.12192

Coles, R. B., Guppy, A., Anderson, M. E. and Schlegel, P. (1989). Frequency sensitivity and directional hearing in the gleaning bat, *Plecotus auritus* (Linnaeus 1758). *J. Comp. Physiol. A* **165**, 269-280. doi:10.1007/BF00619201

Conner, W. E. and Corcoran, A. J. (2012). Sound strategies: the 65-Million-year-old battle between bats and insects. *Annu. Rev. Entomol.* **57**, 21-39. doi:10.1146/annurev-ento-121510-133537

Corcoran, A. J. and Conner, W. E. (2017). Predator counteradaptations: stealth echolocation overcomes insect sonar-jamming and evasive-manoeuvring defences. *Anim. Behav.* **132**, 291-301. doi:10.1016/j.anbehav.2017.08.018

Cummings, M. E. and Endler, J. A. (2018). 25 Years of sensory drive: the evidence and its watery bias. *Curr. Zool.* **64**, 471-484. doi:10.1093/cz/zoy043

Currie, S. E., Boonman, A., Troxell, S., Yovel, Y. and Voigt, C. C. (2020). Echolocation at high intensity imposes metabolic costs on flying bats. *Nat. Ecol. Evol.* **4**, 1174-1177. doi:10.1038/s41559-020-1249-8

de Framond, L., Reininger, V. and Goerlitz, H. R. (2023). Temperate bats may alter calls to partially compensate for weather-induced changes in detection distance. *J. Acoust. Soc. Am.* **153**, 2867. doi:10.1121/10.0019359

Dietz, C. and Kiefer, A. (2016). *Bats of Britain and Europe*. Bloomsbury Publishing.

Dusenbery, D. B. (2001). Physical constraints in sensory ecology. In *Ecology of Sensing* (ed. F. G. Barth and A. Schmid), pp. 1-17. Heidelberg: Springer.

Endler, J. A. (1992). Signals, signal conditions, and the direction of evolution. *Am. Nat.* **139**, S125-S153. doi:10.1086/285308

Fenton, M. B. and Fullard, J. H. (1979). The influence of moth hearing on bat echolocation strategies. *J. Comp. Physiol.* **132**, 77-86. doi:10.1007/BF00617734

Fujioka, E., Aihara, I., Watanabe, S., Sumiya, M., Hiryu, S., Simmons, J. A., Riquimaroux, H. and Watanabe, Y. (2014). Rapid shifts of sonar attention by *Pipistrellus abramus* during natural hunting for multiple prey. *J. Acoust. Soc. Am.* **136**, 3389-3400. doi:10.1121/1.4898428

Goerlitz, H. R. (2018). Weather conditions determine attenuation and speed of sound: Environmental limitations for monitoring and analyzing bat echolocation. *Ecol. Evol.* **8**, 5090-5100. doi:10.1002/ece3.4088

Goerlitz, H. R., ter Hofstede, H. M., Zeale, M. R. K., Jones, G. and Holderied, M. W. (2010). An aerial-hawking bat uses stealth echolocation to counter moth hearing. *Curr. Biol.* **20**, 1568-1572. doi:10.1016/j.cub.2010.07.046

Goerlitz, H. R., ter Hofstede, H. M. and Holderied, M. W. (2020). Neural representation of bat predation risk and evasive flight in moths: A modelling approach. *J. Theor. Biol.* **486**, 110082. doi:10.1016/j.jtbi.2019.110082

Hackett, T. D., Korine, C. and Holderied, M. W. (2014). A whispering bat that screams: bimodal switch of foraging guild from gleaning to aerial hawking in the desert long-eared bat. *J. Exp. Biol.* **217**, 3028-3032. doi:10.1242/jeb.100362

Holderied, M. W. and von Helversen, O. (2003). Echolocation range and wingbeat period match in aerial-hawking bats. *Proc. R. Soc. Lond. B Biol. Sci.* **270**, 2293-2299. doi:10.1098/rspb.2003.2487

Holderied, M. W., Korine, C., Fenton, M. B., Parsons, S., Robson, S. and Jones, G. (2005). Echolocation call intensity in the aerial hawking bat *Eptesicus bottae* (Vespertilionidae) studied using stereo videogrammetry. *J. Exp. Biol.* **208**, 1321-1327. doi:10.1242/jeb.01528

Holderied, M., Korine, C. and Moritz, T. (2011). Hemprich's long-eared bat (*Otonycteris hemprichii*) as a predator of scorpions: whispering echolocation, passive gleaning and prey selection. *J. Comp. Physiol. A* **197**, 425-433. doi:10.1007/s00359-010-0608-3

Hügel, T., van Meir, V., Muñoz-Meneses, A., Clarin, B.-M., Siemers, B. M. and Goerlitz, H. R. (2017). Does similarity in call structure or foraging ecology explain interspecific information transfer in wild *Myotis* bats? *Behav. Ecol. Sociobiol.* **71**, 168. doi:10.1007/s00265-017-2398-x

Jacobs, D. S. and Bastian, A. (2016). Bat echolocation: adaptations for prey detection and capture. In *Predator–Prey Interactions: Co-evolution between Bats and Their Prey* (ed. D. S. Jacobs and A. Bastian), pp. 13-30. Cham: Springer International Publishing.

Jakobsen, L., Brinkløv, S. and Surlykke, A. (2013). Intensity and directionality of bat echolocation signals. *Front. Physiol.* **4**, 89. doi:10.3389/fphys.2013.00089

Jakobsen, L., Hallam, J., Moss, C. F. and Hedenström, A. (2018). Directionality of nose-emitted echolocation calls from bats without a nose leaf (*Plecotus auritus*). *J. Exp. Biol.* **221**, jeb171926. doi:10.1242/jeb.171926

Kawahara, A. Y., Plotkin, D., Espeland, M., Meusemann, K., Toussaint, E. F. A., Donath, A., Gimnich, F., Frandsen, P. B., Zwick, A., dos Reis, M. et al. (2019). Phylogenomics reveals the evolutionary timing and pattern of butterflies and moths. *Proc. Natl. Acad. Sci. USA* **116**, 22657-22663. doi:10.1073/pnas.1907847116

Kohles, J. E., Carter, G. G., Page, R. A. and Dechmann, D. K. N. (2020). Socially foraging bats discriminate between group members based on search-phase echolocation calls. *Behav. Ecol.* **31**, 1103-1112. doi:10.1093/beheco/araa056

Lewanzik, D. and Goerlitz, H. R. (2018). Continued source level reduction during attack in the low–amplitude bat Barbastella barbastellus prevents moth evasive flight. *Funct. Ecol.* **32**, 1251-1261. doi:10.1111/1365-2435.13073

Lewanzik, D. and Goerlitz, H. R. (2021). Task-dependent vocal adjustments to optimize biosonar-based information acquisition. *J. Exp. Biol.* **224**, jeb234815. doi:10.1242/jeb.234815

Lewanzik, D., Sundaramurthy, A. K. and Goerlitz, H. R. (2019). Insectivorous bats integrate social information about species identity, conspecific activity and prey abundance to estimate cost–benefit ratio of interactions. *J. Anim. Ecol.* **88**, 1462-1473. doi:10.1111/1365-2656.12989

Møhl, B. (1988). Target detection by echolocating bats. In *Animal Sonar*, pp. 435-450. Springer.

Morales, A. E., Ruedi, M., Field, K. and Carstens, B. C. (2019). Diversification rates have no effect on the convergent evolution of foraging strategies in the most speciose genus of bats, *Myotis*. *Evolution* **73**, 2263-2280. doi:10.1111/evo.13849

Norberg, U. M., Rayner, J. M. V. and Lighthill, M. J. (1987). Ecological morphology and flight in bats (Mammalia; Chiroptera): wing adaptations, flight performance, foraging strategy and echolocation. *Philos. Trans. R. Soc. Lond. B. Biol. Sci.* **316**, 335-427. doi:10.1098/rstb.1987.0030

Obrist, M. K. and Boesch, R. (2018). BatScope manages acoustic recordings, analyses calls, and classifies bat species automatically. *Can. J. Zool.* **96**, 939-954. doi:10.1139/cjz-2017-0103

Pedersen, S. C. (1998). Morphometric analysis of the chiropteran skull with regard to mode of echolocation. *J. Mammal.* **79**, 91-103. doi:10.2307/1382844

Pedersen, S. C. and Müller, R. (2013). Nasal-emission and nose leaves. In *Bat Evolution, Ecology, and Conservation* (ed. R. A. Adams and S. C. Pedersen), pp. 71-91. New York, NY: Springer New York.

Ratcliffe, J. M. and Dawson, J. W. (2003). Behavioural flexibility: the little brown bat, *Myotis lucifugus*, and the northern long-eared bat, *M. septentrionalis*, both glean and hawk prey. *Anim. Behav.* **66**, 847-856. doi:10.1006/anbe.2003.2297

Roeder, K. D. and Treat, A. E. (1957). Ultrasonic reception by the tympanic organ of noctuid moths. *J. Exp. Zool.* **134**, 127-157. doi:10.1002/jez.1401340107

Russ, J. (2012). *British Bat Calls: a Guide to Species Identification*. Pelagic Publishing.

Rydell, J. (1989). Food habits of northern (*Eptesicus nilssoni*) and brown long-eared (*Plecotus auritus*) bats in Sweden. *Holarct. Ecol.* **12**, 16-20.

Seibert, A.-M., Koblitz, J. C., Denzinger, A. and Schnitzler, H.-U. (2015). Bidirectional echolocation in the bat *Barbastella barbastellus*: different signals of low source level are emitted upward through the nose and downward through the mouth. *PLoS One* **10**, e0135590. doi:10.1371/journal.pone.0135590

Shiel, C. B., McAney, C. M. and Fairley, J. S. (1991). Analysis of the diet of Natterer's bat *Myotis nattereri* and the common long-eared bat *Plecotus auritus* in the West of Ireland. *J. Zool.* **223**, 299-305. doi:10.1111/j.1469-7998.1991.tb04766.x

Stidsholt, L., Greif, S., Goerlitz, H. R., Beedholm, K., Macaulay, J., Johnson, M. and Madsen, P. T. (2021). Hunting bats adjust their echolocation to receive weak prey echoes for clutter reduction. *Sci. Adv.* **7**, eabf1367. doi:10.1126/sciadv.abf1367

Stidsholt, L., Hubancheva, A., Greif, S., Goerlitz, H. R., Johnson, M., Yovel, Y. and Madsen, P. T. (2022). Echolocating bats prefer a high risk-high gain foraging strategy to increase prey profitability. *Elife* **12**, e84190. doi:10.7554/eLife.84190

Stilz, W.-P. and Schnitzler, H.-U. (2012). Estimation of the acoustic range of bat echolocation for extended targets. *J. Acoust. Soc. Am.* **132**, 1765-1775. doi:10.1121/1.4733537

Surlykke, A. (1988). Interaction between echolocating bats and their prey. In *Animal Sonar: Processes and Performance* (ed. P. E. Nachtigall and P. W. B. Moore), pp. 551-566. Boston, MA: Springer US.

Surlykke, A. and Kalko, E. K. (2008). Echolocating bats cry out loud to detect their prey. *PLoS One* **3**, e2036. doi:10.1371/journal.pone.0002036

Surlykke, A., Boel Pedersen, S. and Jakobsen, L. (2009). Echolocating bats emit a highly directional sonar sound beam in the field. *Proc. R. Soc. B Biol. Sci.* **276**, 853-860. doi:10.1098/rspb.2008.1505

Szewczac, J. M. (2004). Advanced analysis techniques for identifying bat species. In *Bat echolocation Research: Tools, Techniques & Analysis*, pp. 121-127. Austin, Texas: Bat Conservation International.

Ter Hofstede, H. M. and Ratcliffe, J. M. (2016). Evolutionary escalation: the bat–moth arms race. *J. Exp. Biol.* **219**, 1589-1602. doi:10.1242/jeb.086686

Vesterinen, E. J., Puisto, A. I. E., Blomberg, A. S. and Lilley, T. M. (2018). Table for five, please: Dietary partitioning in boreal bats. *Ecol. Evol.* **8**, 10914-10937. doi:10.1002/ece3.4559

Waters, D. A. and Jones, G. (1995). Echolocation call structure and intensity in five species of insectivorous bats. *J. Exp. Biol.* **198**, 475-489. doi:10.1242/jeb.198.2.475

Wotton, J. M., Haresign, T. and Simmons, J. A. (1995). Spatially dependent acoustic cues generated by the external ear of the big brown bat, *Eptesicus fuscus*. *J. Acoust. Soc. Am.* **98**, 1423-1445. doi:10.1121/1.413410

Yin, X. and Müller, R. (2019). Fast-moving bat ears create informative Doppler shifts. *Proc. Natl. Acad. Sci. USA* **116**, 12270-12274. doi:10.1073/pnas.1901120116

Supplementary Materials and Methods

Calibration of the sensitivity of the central microphone

To analyse calls as they were emitted by the bat, call recordings need to be corrected for microphone characteristics. We thus measured the frequency- and direction-dependent sensitivity of the central microphone of the array. We broadcast a calibration sound (1 sec of band-limited white noise (6-95 kHz) and 100-ms pure tones from 6 kHz to 95 kHz in steps of 1 kHz, all corrected for the frequency response of the loudspeaker) from a loudspeaker (custom-built Polaroid speaker). The loudspeaker was placed at 50 cm distance to a ¼-inch measuring microphone with flat frequency response (40BF, with preamplifier 26AC and power module 12AA; GRAS Sound and Vibration, Holte, Denmark) and to the microphone used for recording the bat calls in the field (FG-O, Avisoft Bioacoustics, Glienicke, Germany). The sensitivity of the measuring microphone was calibrated by recording a 1 kHz tone at 94 dB SPL rms (sound calibrator 4231, Brüel & Kjaer, Nærum, Denmark).

Accuracy of 3D-localization and source-level calculations

We performed two calibration measurements to determine the accuracy of our acoustic tracking system (consisting of our array and the TOADSuite software package) for calculating (i) the 3D-coordinates of bats and (ii) the (apparent) source levels of bat calls. As acoustic signals for calibration, we used two types of echolocation-like signals: a linear downward frequency-modulated sweep (FM, 90-25 kHz), and a logarithmic downward frequency-modulated sweep (mimicking a FM-QCF call of e.g., pipistrelle bats; 90-25 kHz). Each signal was generated with three different durations (3, 6, and 9 ms) with a Hann window (to avoid clicks in the loudspeaker) and repeated five times, so that the total playback comprised 30 sweeps, sandwiched between two 100-ms long audible pure tones of 10 kHz (total playback duration 4.8 sec) to indicate the start and end of a playback sequence. The ramp segment of the Hann window is dependent on the total duration of the sound and thus varies with the signal durations. Hence the measured signal duration at -12 dB below peak amplitude will be lower than the specified values.

First, we broadcast this playback from a loudspeaker (custom-built Polaroid speaker) at 3, 4.5, 6, 8.5, and 10 m distance to the microphone array in a large hall. In addition to the on-axis recording (i.e., 0° azimuth and elevation), we also rotated the array relative to the loudspeaker to record the playback from 30° and 60° off-axis in both elevation (below the array's central axis) and azimuth (to the left of the array's central axis). We measured the

distance between the microphone and the loudspeaker with a laser range-finder (GLM 50C, Bosch, Germany) for every distance and angle adjustment. In total, we thus recorded 1,350 sweeps (30 sweeps per broadcast (2 sweeps × 3 durations × 5 repetitions) × 5 distances × 3 directions in azimuth × 3 directions in elevation).

Second, we analysed the array recordings of the calibration playback with the TOADSuite in the same way as the bat calls recorded in the field (see main text). In short, we band-pass-filtered the recordings (18-90 kHz), automatically detected the broadcast sweeps, determined the time-of-arrival-differences of each sweep between the microphones by cross-correlation, calculated each sweep's three-dimensional position, compensated the sweep's recorded waveform for the frequency- and direction-dependent microphone sensitivity and for the distance-dependent geometric and atmospheric attenuation, and then calculated each sweep's source level from the compensated waveform (both as peak-equivalent SPL and RMS-SPL). This resulted in the 3D-position and source levels of the calibration playback as calculated by the TOADSuite, which we compared in the next steps to the real 3D-positions (as measured by the laser range finder, see above) and the real source level (as calibrated with a measuring microphone, see next step).

Third, we measured the real source level of our playbacks with a calibrated ¼-inch measuring microphone with flat frequency response (40BF, with preamplifier 26AC and power module 12AA; GRAS Sound and Vibration, Holte, Denmark) in an echo-attenuated room. We placed the Polaroid loudspeaker at 50 cm to the measuring microphone and recorded the playback consisting of 30 sweeps. We used custom-written scripts (provided online) in R version 3.6.1 (R Core Team, 2019) to analyse the calibration recording in the same way as the TOADSuite to obtain the real source levels of our playback. Specifically, we band-pass-filtered the recording (18-90 kHz), detected the 30 sweeps, and calculated for each sweep its peak-amplitude from the envelope of the waveform and the RMS-value of the waveform within the -12 dB call duration criterion. By comparing these amplitude measurements to the recording of a calibration tone (94 dB SPL rms, 1 kHz; sound calibrator 4231, Brüel & Kjaer, Nærum, Denmark), we calculated the real source level of both sweeps, both as peak-equivalent value and RMS value, expressed in dB SPL re. 20 µPa at 10 cm distance.

3D Location:

We determined the accuracy of our acoustic tracking system to calculate the three-dimensional coordinates and the source level of a sound source. From the reconstructed 3D-position of the loudspeaker, we calculated the reconstructed distance between loudspeaker

and central microphone. To quantify the spatial accuracy of our acoustic tracking system, we compared the reconstructed distance to the real distance that we measured with the laser range finder. We express the spatial error between the reconstructed and real distance as the percentage of the absolute difference between the reconstructed and real distance, relative to the real distance:

(1)   spatial error (%) = (reconstructed_distance – real_distance) / real_distance * 100.

The effects of the different variables (Distance to the array, Azimuth, Elevation, call duration, call design) on the error in sound source localisation and source level were estimated using a Gaussian Generalized Linear Model (GLM) with identity link function in a Bayesian framework (package *rstanrm* v. 2.21.3, in R v. 4.2.2). Four chains of 5000 iteration each were run (warmup 2500 iteration, thinning rate 1) using the default normal non-informative prior. We examined the quality of model fit following (Gabry, 2022) (package *bayesplot* v. 1.10.1) by examining the MCMC trace, ensuring the Rhats and effective sample size were acceptable, and ensuring that there was minimum autocorrelation within each chain.

The overall mean localization error was close to Zero (-0.5% of the real distance), with a standard-deviation of 4.1% and a range from -9.4 – 10.9% (**Fig. S1**). This small mean error indicates that the tracking system does not systematically over- or underestimate the real position. Calculating a smoothed trajectory of the noisy raw data will thus likely result in a good estimate of the real flight trajectory, and excluding raw data points that are more than ~10% off the smoothed trajectory appears to be justified.

The loudspeaker localization error was independent of the call type (FM or FM-QCF, GLM mean estimate and 95% credible interval: ß (FM-qCF) = -0.91 % [-1.19, -0.63]), and not strongly affected by the azimuth and elevation of the loudspeaker. Generally, the calculated source distance increases with larger elevational off-axis angles (**Fig. S1**, ß(30°) = 2.32% [1.98, 2.66], ß(60°) = 5.36% [5.01, 5.70]) and with smaller azimuthal off-axis-angles (**Fig. S1**, ß(30°) = -1.44% [-1.81, -1.11], ß(60°) = -4.87% [-5.22, -4.51]). The error in localisation caused by distance, elevation and azimuth were all within 6% of the real distance. The distance of the sound source had the most notable effect, causing increasing dispersion of the error, which can likely be attributed to decreasing signal-to-noise ratio (SNR).

In addition to calculating the error for the overall distance, we performed the same calculations separately for each of the three spatial dimensions (X, Y, Z), i.e., we express the spatial error for each dimension by comparing the reconstructed distance to the real distance in that dimension. The X- and Z-axes form the plane of the microphone array, with X being the horizontal and Z the vertical axis, and the Y-axis is the direction away from the array.

Analysing the distance error separately for the three axes showed similar mean errors (±SD) of -1.3±3.9% along the X-coordinate, -1.1±5.8% along the Y-coordinate (distance) and 0.3±5.1% along the Z-coordinate (height). The range of the errors was largest along the distance-axis (Y-coordinate), which is expected for 3D-triangulation methods: X-range = -10.3 – 9.3%, Y-range = -25.5 – 11.2%, Z-range = -13.6 – 10.8%.

Source Level: To quantify the acoustic accuracy of our acoustic tracking system in measuring source levels, we compared the reconstructed source level (SL) to the real source level obtained from the measuring microphone. We express the accuracy of source level reconstruction as the difference between reconstructed and real source level:

(2)   SL error (dB) = reconstructed_SL – real_SL.

We used the same statistical method to analyse the effect of call type and distance to the microphone as explained int eh previous section. The mean source levels of our playback signals (relative to 20 µPa and at 10 cm distance to the loudspeaker) were 115.1 dB peSPL (111.8 dB SPL RMS) for the FM signal, and 110.1 dB peSPL (106.1 dB SPL RMS) for FM-QCF signals (±0.1 dB SD in all cases for the 15 sweeps per call type). The source levels calculated by the TOADSuite were slightly lower than these values, resulting in a mean (±SD) source level error of -1.1±1.7 dB for peSPL and -4.2±1.5 dB for rmsSPL (**Fig. S2**). The source level error was independent of the call type (GLM estimates and 95% Credible interval: ß(FM-qCF) =   -0.12 dB [-0.25, 0.01]) and the distance to the microphone (ß(distance) = 0.13 dB/m [0.10, 0.15]).
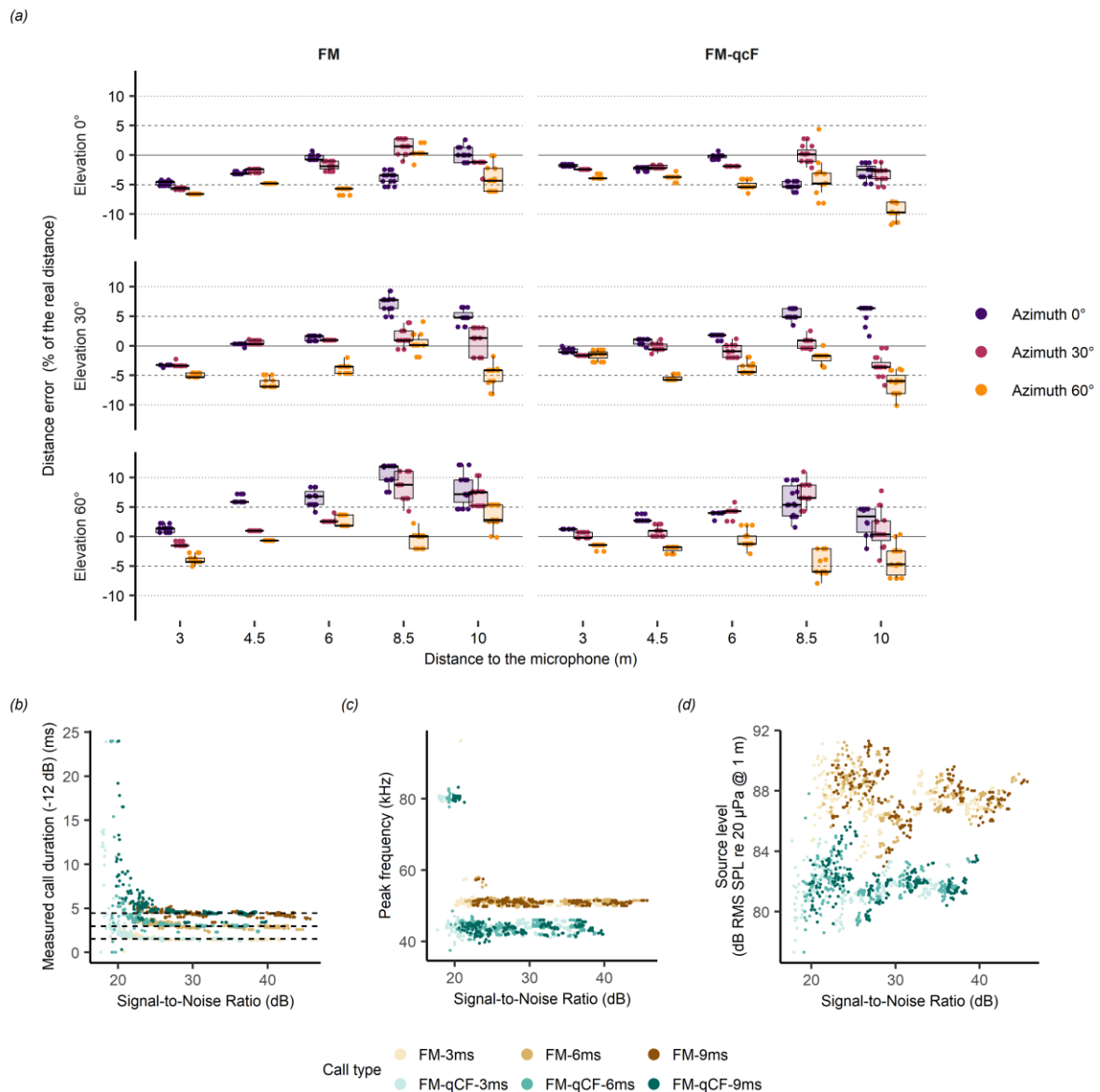
Fig. S1. Accuracy of measuring 3D-positions (A) and call parameters (B-D) with a 60-cm star-shaped microphone array and the TOADSuite

a) The tracking accuracy is indicated by the distance error, which is the difference between the distance calculated with the TOADSuite and the real distance measured with the laser range finder, expressed as a percentage of the real distance. Data is presented as a function of the distance to the microphone, and separated by elevation (panels from top to bottom) and azimuth (color-coded), for two call types (FM signals, left, and FM-QCF signals, right). Raw data is shown behind boxplots, which show median, quartiles, and 95th-percentiles.

b) Measured call duration as a function of the signal-to-noise-ratio. Signal duration and shape are coded with shades and colours. As comparison, the dashed lines show calculated durations for the playback at 1 m distance and recorded with a measurement microphone and analysed independently in R using the same method implemented in the TOADSuite. Note

that the durations measured with the TOADSuite match the durations on the original playback at high signal to noise levels, but reach unrealistic values when the signal to noise level is below 20 dB.

c) Measured peak frequency as a function of the signal to noise ratio. The peak frequency of the FM-QCF signal is rather constant around 45 kHz because of the long CF component in the call. The FM signals have a peak frequency around 50 kHz because this is the frequency that is most intense after accounting for windowing, and perhaps as a result of the speaker frequency response.

d) Source level calculated with the TOADSuite as a function of the signal to noise ratio.

In summary, source level estimates for peak-values are quite accurate (-1 dB) when averaged over sufficient calls, while the error is larger for average (RMS) estimates (-4 dB). Lower signal-to-noise ratios increased the error but did not lead to any systematic bias in source level measurements (**Fig. S1 D**).

Potential reasons for the larger error in RMS-estimates might be fluctuations in the call envelope caused by interference patterns under real-world recording conditions, incomplete compensation of the microphone's frequency response, and other unknown effects.

Call duration and frequency of calls recorded in the field

The call duration and frequency parameters show some variation and a few outliers (**Fig. 3C**). Analysing call duration as a function of the signal-to-noise ratio (SNR) showed that the call durations and frequencies are reliable for SNR above ~20 dB. For SNR <20 dB, the call duration and frequency of some (but not all) sweeps increased, yet with no obvious pattern regarding which sweep was affected, and no difference between FM and FM-QCF sweeps (**Fig. S1 B,C**). One reason for this pattern might be that with decreasing SNR, the call definition threshold (-12 dB re. maximum amplitude) falls below random fluctuations of the envelope and thus includes noise into the call definition, explaining the few very high call durations in **Fig. 3**.

Overall, we did not find any pattern explaining the extreme outliers in duration and frequency (e.g., long-eared bat calls with long duration were not the same as the calls with very high peak frequency or lowest frequency; no pattern in SNR or localization error) and thus included all data into the analysis.

Table S1. Individual median (quartiles in brackets below) echolocation call parameters for each bat. N: Number of analysed echolocation calls per bat. aSL: apparent source level (re 20µPa) at 10 cm in front of the bat. We recorded one peak frequency for each call, which sometimes was in the first harmonic, and sometimes in the second harmonic. We grouped calls based on their peak frequency (<50 kHz the measured peak frequency was in the first harmonic, H1, and >50 kHz, the measured peak frequency was in the second harmonic, H2). LoF: lowest frequency.

| Bat ID	N	Apparent Source level (dB peSPL)	(dB SPL rms)	duration (ms)	Peak frequency (kHz) H1	H2	LoF (kHz)
5274	33	88.9 (86.9-91.6)	82.4 (80.1-85.1)	1.9 (1.6-2.2)	37.8 (33.6-40.4)	64.0 (62.6-68.9)	26.5 (24.7-27.8)
5280	19	88.3 (86.2-90.4)	82.3 (78.9-84.0)	2.7 (2.1-4.9)	31.8 (29.5-33.3)	79.3 (78.8-79.8)	22.3 (21.8-22.7)
5295	17	91.2 (84.2-93.4)	84.0 (77.3-86.4)	1.9 (1.7-2.2)	39.0 (37.9-42.1)	65.5 (64.9-77.7)	28.3 (25.3-32.3)
5297	13	96.6 (88.2-97.9)	89.1 (81.4-92.0)	3.1 (2.5-3.9)	33.0 (32.3-37.9)	64.9 (63.5-79.0)	29.8 (27.8-50.2)
5298	16	94.9 (91.7-99.0)	87.9 (84.2-92.6)	2.5 (2.3-2.8)	39.0 (37.8-39.8)	79.9 (79.5-80.3)	24.8 (23.9-26.1)
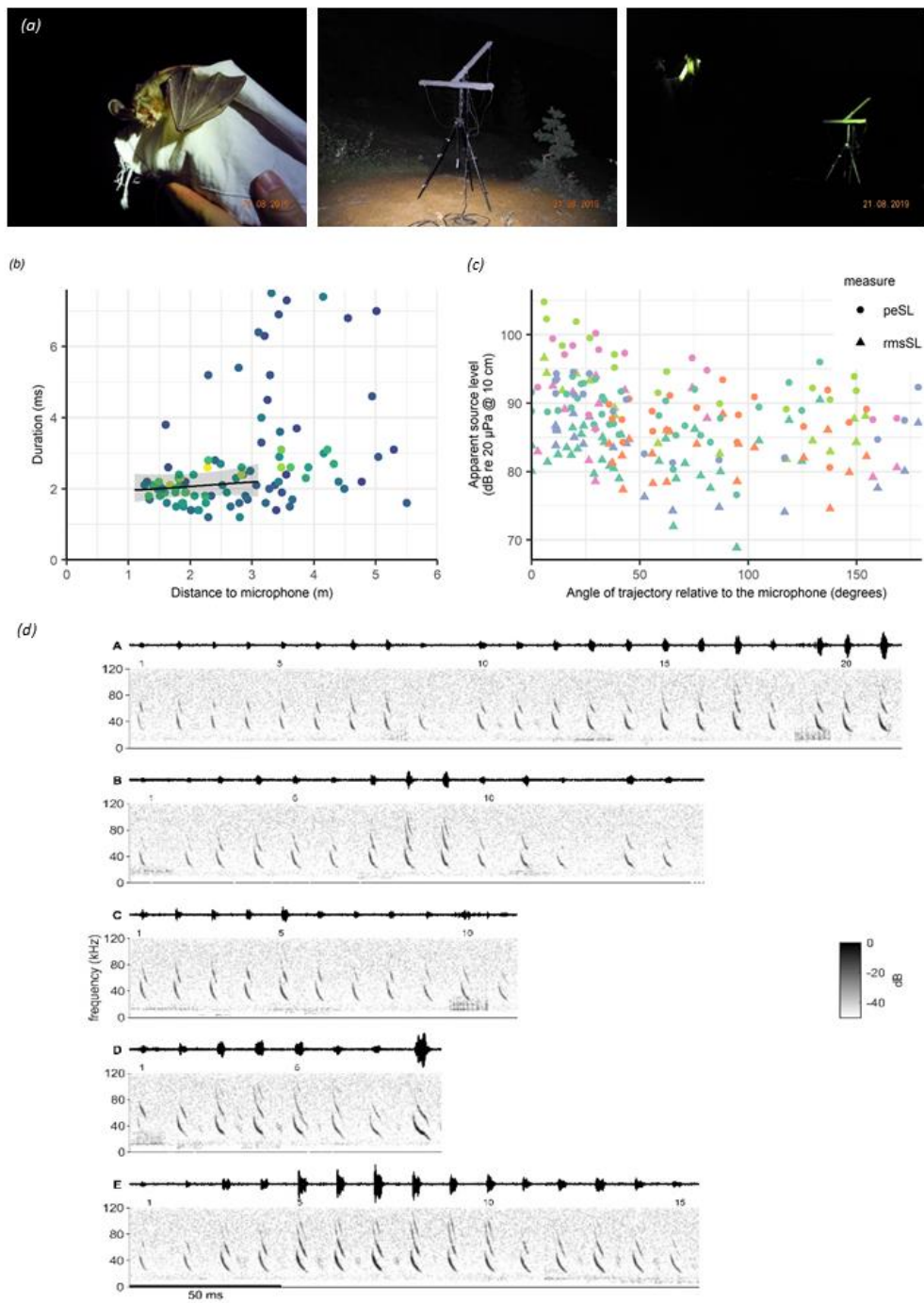
Fig. S2. Experimental situation, effect of flight behaviour on call parameters and recorded calls.

a) From left to right, one individual of a brown-long-eared bat, *Plecotus auritus*, before release, the microphone array in the field (note the open surroundings), and hand release of one individual (left) in front of the microphone array (right).

b) Effect of the distance between the bat and the microphone array on call duration. Raw data points are color-coded according to the signal to noise ratio. Note that many points

have a very low signal to noise ratio (<20 dB) at distances >3 m from the microphone array, which are also the calls with high call duration and frequency. Within 3 m of the microphone array (where the signal to noise ratio is high for most calls), the call duration did not change with distance to the array (Linear Mixed Effect Model of the log (call duration) as a function of distance to the array, bat identity as a random effect, ß(distance) = 0.06, 95% credible interval [-0.09, 0.20], that is an increase by .2 ms on average over 3 m).

c) Source level as a function of the angle between direction from the bat to the microphone array and the bat's actual flight direction, color-coded per individual.

d) Waveforms (top) and spectrograms (bottom) of the analysed calls of the five bats. Note that for better visibility, only the concatenated individual detected and analysed calls are shown, not the complete recorded call sequences including silent phases between calls. The letters refer to bat identity in Figure 2 in the main manuscript.

Supplementary References

Gabry, J. (2022). Graphical posterior predictive checks using the bayesplot package.

Gabry, J. and Mahr, T. (2022). bayesplot: Plotting for Bayesian Models.

Goodrich, B., Gabry, J., Ali, I. and Brilleman, S. (2020). rstanarm: Bayesian applied regression modeling via Stan.

R Core Team (2019). R: A language and environment for statistical computing.